Tetracoordinated Manganese(III) Alkylcorrolates. Spectroscopic Studies and the Crystal and Molecular Structure of (7,13-Dimethyl-2,3,8,12,17,18-hexaethylcorrolato)manganese(III)

Silvia Licoccia,*,† Elisabetta Morgante,† Roberto Paolesse,† Francesca Polizio,‡ Mathias O. Senge,§ Eugenio Tondello,|| and Tristano Boschi†

Dipartimento di Scienze e Tecnologie Chimiche and Dipartimento di Biologia, Università di Roma Tor Vergata, Via della Ricerca Scientifica, 00133 Rome, Italy, Institut für Organische Chemie (WE02), Freie Universität, Takustrasse 3, D-14195 Berlin, Germany, and Dipartimento di Chimica Inorganica, Metallorganica ed Analitica, Università di Padova, Via Loredan 4, 35131 Padua, Italy

Received March 28, 1996[⊗]

(2,3,7,8,12,13,17,18-Octamethylcorrolato)manganese(III), [Mn(OMC)], has been characterized by several physical measurements. In the presence of nitrogenous bases the complex exists as a valence tautomer [$Mn^{II}(OMC^{\bullet+})$] as demonstrated by ^{1}H NMR and EPR. Complete resonance assignment in the NMR spectrum has been achieved by systematic substitution of the peripheral substituents. The crystal structure of the first example of a tetracoordinated tetrapyrrolic macrocycle Mn(III) complex, (7,13-dimethyl-2,3,8,12,17,18-hexamethylcorrolato)-manganese(III), [Mn-7,13-Me_2-HEC)], is also reported. Crystal data with Cu Kα (λ = 1.541 78 Å) at 293 K are as follows: $C_{33}H_{39}MnN_4$, a = 4.671(2) Å, b = 28.31(2) Å, c = 20.882(6) Å, β = 94.60(3)°, V = 2753(2) Å^3, Z = 4, monoclinic, space group $P2_1/n$, 4088 data, $R1$ = 0.0563 for 4088 observed reflections with $I > 2\sigma(I)$. The analysis reveals a high degree of planarity of the macrocycle and the existence of strong overlap between the π systems with the formation of an infinite stack of molecules.

Introduction

Among the various tetrapyrrolic macrocycles corrole is a particularly interesting one because of its structure that can be considered as intermediate between that of the porphyrin, the prosthetic group of hemoproteins, and that of corrin, the nucleus of vitamin B_{12} coenzyme. It has, in fact, a corrin-like molecular skeleton, with a direct link between two pyrrole rings and a porphyrin-like 18 electron π system. Corrole is then aromatic as confirmed by its electronic and NMR spectra. It is a very versatile ligand capable of coordinating several main group and transition metals. Synthetic and spectroscopic studies carried out on metal derivatives of corrole have shown that its ligand field substantially differs from that of other macrocycles.[1]

To gain a better understanding of the metal−macrocycle bond we have now extended our investigations to manganese corrolates.

Manganese is present in numerous biological systems: by variation of its oxidation and ligation states it mediates several biological functions.[2,3] Furthermore manganese complexes have been successfully used as catalysts for the mild homogeneous oxidations of different organic functions.[4,5]

In a previous paper we have reported on the synthesis of the manganese derivative of 2,3,7,8,12,13,17,18-octamethylcorrole (H_3OMC). The complex was characterized by elemental analyses and electronic spectroscopy and formulated as [Mn-(OMC)].[6]

Since coordination number 4 is very unusual for Mn(III) complexes, we have now carried out several physical measurements to further characterize manganese corrolates and define the metal coordination number and geometry without ambiguity. We then report the synthesis and spectroscopic characterization of several Mn(III) corrolates, which structural formulas are reported in Figure 1, where the peripheral substituents have been varied in order to obtain higher solubility, achieve complete resonance assignment in their ^{1}H NMR spectra, and define the origin of the isotropic shift. Their axial ligand binding properties in solution have also been investigated.

Experimental Section

Electronic spectra have been recorded on a Philips PU8700 spectrophotometer.

Electron impact mass spectra were recorded on a VG QUATTRO spectrometer.

X-ray photoelectron spectra were run on a Perkin-Elmer PHI 5600ci spectrometer employing an Al Kα source ($h\nu$ = 1486.6 eV). The working pressure was 2×10^{-8} Pa. The spectrometer was calibrated by assuming the binding energy (BE) of the Au $4f_{7/2}$ line at 83.9 eV with respect to the Fermi level. The C 1s line of adventitious carbon was assumed at 248.8 eV as internal reference for peak positions. The uncertainty is ±0.1 eV.

EPR spectra were recorded at 100 K on a Bruker ESP 300 spectrometer operating at 9.44 GHz microwave frequency, 100 KHz field modulation, 20 mW microwave power, and 0.1 mT modulation amplitude; g values were calculated using diphenylpicryl hydrazyl (dpph) as calibrant. The concentrations of the samples ranged from 5×10^{-2} to 5×10^{-4} M.

Room-temperature susceptibility measurements were obtained by the Gouy method on a permanent magnet (0.7 T) by using a solution of

† Dipartimento di Scienze e Tecnologie Chimiche, Università di Roma Tor Vergata.
‡ Dipartimento di Biologia, Università di Roma Tor Vergata.
§ Freie Universität.
|| Università di Padova.
⊗ Abstract published in *Advance ACS Abstracts,* March 1, 1997.

(1) Licoccia, S.; Paolesse, R. In *Metal Complexes with Tetrapyrrole Ligands III*; Buchler, J. W., Ed.; Springer-Verlag: Berlin and Heidelberg, Germany, 1995.
(2) Bertini, I.; Luchinat, C. In *NMR of Paramagnetic Molecules in Biological Systems*; Lever, A. B. P., Gray, H. B., Eds.; The B. Cummings Publ. Co.: Menlo Park, CA, 1986.
(3) Larson, E. J.; Pecoraro, V. L. In *Manganese Redox Enzymes*; Pecoraro, V. L., Ed.; VCH Publishers Inc.: New York, 1992.
(4) Stern, M. K.; Groves, J. T. In *Manganese Redox Enzymes*; Pecoraro, V. L., Ed.; VCH Publishers Inc.: New York, 1992.
(5) *Metalloporphyrins in Catalytic Oxidations*; Sheldon, R. A. Ed.; Marcel Dekker Inc.: New York, 1994.
(6) Boschi, T.; Licoccia, S.; Paolesse, R.; Tehran, M. A.; Pelizzi, G.; Vitali, F.; *J. Chem. Soc., Dalton Trans.* **1990**, 463.

S0020-1669(96)00334-5 CCC: $14.00

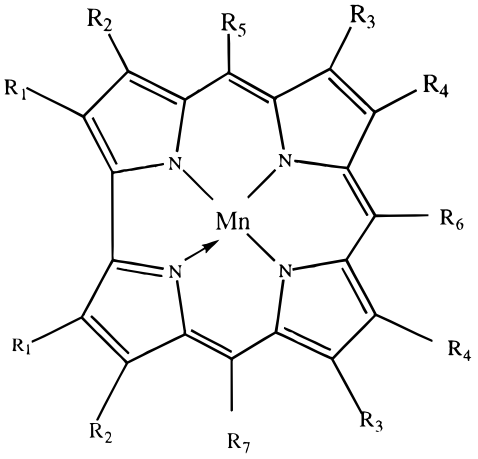

Figure 1. Structural formulas of manganese corrolates: **1**, [Mn(OMC)] ($R_5 = R_6 = R_7 = H$; $R_1 = R_2 = R_3 = R_4 = CH_3$); **2**, [Mn(3,17-$Et_2$-HMC)] ($R_5 = R_6 = R_7 = H$; $R_2 = CH_2CH_3$; $R_1 = R_3 = R_4 = CH_3$); **3**, [Mn(7,13-Et_2-HMC)] ($R_5 = R_6 = R_7 = H$; $R_3 = CH_2CH_3$; $R_1 = R_2 = R_4 = CH_3$); **4**, [Mn(8,12-Et_2-HMC)] ($R_5 = R_6 = R_7 = H$; $R_4 = CH_2CH_3$; $R_1 = R_2 = R_3 = CH_3$); **5**, [Mn(7,8,12,13-TMC)] ($R_5 = R_6 = R_7 = H$; $R_3 = R_4 = H$; $R_1 = R_2 = CH_3$); **6**, [Mn(7,13-Me_2-HEC)] ($R_5 = R_6 = R_7 = H$; $R_3 = CH_3$; $R_1 = R_2 = R_4 = CH_2CH_3$); **7**, [Mn(5,15-^{2}H-8,12-Et_2-HMC)] ($R_5 = R_7 = {}^2H$; $R_6 = H$; $R_1 = R_2 = R_3 = CH_3$; $R_4 = CH_2CH_3$).

$NiCl_2$ as calibrant. Diamagnetic corrections for ligand contribution were applied by using Pascal's constants.

A Bruker AM 400 spectrometer operating in the quadrature mode was used to obtain ^{1}H NMR spectra. All chemical shifts are given in ppm from tetramethylsilane (TMS) and are referenced against residual solvent signals. Typical spectra consisted of 1024−2048 transients of 8192 data points over a 167 kHz bandwidth using a 5.8 ms 90° pulse. The concentrations of the complexes were in the range 10^{-2}−10^{-4} M.

Nonselective spin−lattice relaxation rates were obtained using the standard (180°−τ−90°) inversion recovery method with a repetition rate of 1.5 s^{-1}. T_1 relaxation times were calculated from semilogarithmic plots prepared from spectra consisting of 256 scans. Mean square errors did not exceed 10%. T_2 spin−spin relaxation times were estimated from the half-height line width of the resonances.

Magnetic susceptibilities in solution were determined according to literature methods.[7,8] Magnetic moments have been calculated by following published procedure.[9]

All chemicals (Carlo Erba Reagenti) were reagent grade and were used without further purification.

Mn corrolates **1**−**7** have been prepared by following the published procedure.[6]

Synthesis of 3,4-Dimethyl-2-[^{2}H]formylpyrrole (8). Phosphorus oxychloride (2.2 mL, 22 mmol) was added dropwise to a solution of [^{2}H]$_7$-*N*,*N*-dimethylformamide (2 mL, 26 mmol) in dichloromethane (10 mL). The mixture was stirred at 0 °C for 15 min and then added to a solution of 3,4-dimethylpyrrole[10] in dichloromethane (40 mL). The new solution was stirred for 3 h at room temperature. Saturated aqueous sodium carbonate (100 mL) was then added, and the mixture was stirred overnight. The organic phase was extracted with dichloromethane and dried over sodium sulfate, and the solvent was vacuum evaporated. The residue was chromatographed on silica gel (dichloromethane as eluant) and the appropriate fraction collected and crystallized from *n*-hexane to afford 1.9 g (71%) of the title compound.

^{1}H NMR: δ 9.68 (br s, 1 H), 6.98 (s, 1 H), 2.19, 1.93 (each s, 6 H). Anal. Calcd for C_7H_9NO: C, 68.27; H, 7.37; N, 11.37. Found: C, 68.03; H, 7.16; N, 11.56.

Synthesis of Biladienes. 8,12-Diethyl-2,3,7,13,17,18-hexamethylbiladiene-*a*,*c* dihydrobromide (**9**), 3,17-diethyl-2,7,8,12,13,18-hexamethylbiladiene-*a*,*c* dihydrobromide (**10**), and 7,13-dimethyl-2,3,8,-12,17,18-hexaethylbiladiene-*a*,*c* dihydrobromide (**11**) were prepared according to literature methods.[11,12]

8,12-Diethyl,-2,3,7,13,17,18-hexamethyl-5,15-[^{2}H]$_2$-biladiene-*a*,*c* Dihydrobromide (12). 2,3,7,8-Tetramethyldipyrromethane-1,9-dicarboxylic acid[13] (500 mg, 1.7 mmol) was stirred in trifluoroacetic acid (5 mL) for 10 min before being treated with a solution of **8** (430 mg, 3.5 mmol) in methanol (20 mL) along with 3 mL of 31% HBr in acetic acid. Diethyl ether was added until the precipitation of the biladiene-*a*,*c* was complete; the mixture was filtered off, washed with diethyl ether and air dried yielding 808 mg (78%) of the labeled biladiene-*a*,*c*.

UV−vis: λ_{max} 461 nm (ϵ 62 000), 521 (134 000). ^{1}H NMR: δ 13.48, 13.32 (each br s, 4 H), 7.83 (d, 2 H), 5.12 (s, 2 H), 2.56 (q, 4 H), 2.34, 2.08 (each s, 18 H), 0.94 (t, 6 H). Anal. Calcd for $C_{29}H_{38}Br_2N_4$: C, 57.82; H, 6.36; N, 9.30. Found: C, 58.03; H, 6.16; N, 9.07.

7,13-Diethyl-2,3,8,12,17,18-hexamethylbiladiene-*a*,*c* Dihydrobromide (13). Treatment of 2,8-diethyl-3,7-dimethyldipyrromethane-1,9-dicarboxylic acid[14] (500 mg, 1.6 mmol) and 3,4-dimethyl-2-formylpyrrole[15] (406 mg, 3.3 mmol) by following the procedure described above afforded 860 mg (83%) of the title compound.

UV−vis: λ_{max} 465 nm (ϵ 136 000), 523 (93 000). ^{1}H NMR: δ 13.34, 13.18 (each br s, 4 H), 8.01 (d, 2 H), 7.34 (s, 2 H), 5.20 (s, 2 H), 2.75 (q, 4 H), 2.35, 2.25 (each s, 18 H), 1.28 (t, 6 H). LR-FAB MS: *m*/*z* 602 (M^+). Anal. Calcd for $C_{29}H_{38}Br_2N_4$: C, 57.82; H, 6.36; N, 9.30. Found: C, 58.03; H, 6.16; N, 9.07.

7,8,12,13-Tetramethylbiladiene-*a*,*c* Dihydrobromide (14). Treatment of 2,3,7,8-tetramethyldipyrromethane-1,9-dicarboxylic acid (500 mg, 1.7 mmol) and 2-formylpyrrole (330 mg, 3.5 mmol) with the same synthetic procedure afforded 562 mg (63%) of the title compound. The compound decomposed when dissolved in $CHCl_3$.

UV−vis: λ_{max} 441 nm (ϵ 115 000), 506 (63 000). LR FAB MS: *m*/*z* 429 (M^+). Anal. Calcd for $C_{23}H_{26}Br_2N_4$: C, 53.30; H, 5.06; N, 10.81. Found: C, 52.96; H, 5.36; N, 10.27.

X-ray Crystallographic Study. The crystals were grown by slow diffusion of a 99:1 dichloromethane/pyridine solution of the complex into *n*-hexane. A suitable crystal was selected, attached to a glass fiber, and mounted on a Siemens R3m/V diffractometer. Data were collected at 293 K using Cu Kα radiation (λ = 1.541 78 Å). Three standard reflections were measured every 150 reflections and showed only statistical variation of the intensity (<1.5%). The intensities were corrected for Lorentz and polarization effects; extinction was disregarded. Crystallographic programs used for the structure solution and refinement were those of the SHELXTL-Plus program installed on a PC clone.[16] Scattering factors were those provided with the SHELXTL-Plus program system. Some details of the data collection and refinement are given in Table 1, atomic coordinates are provided in Table 2, and important bond lengths and angles are given in Table 3. Further details are provided in the Supporting Information.

The structure was solved by direct methods; missing atoms were located in difference Fourier maps. The structure was refined by full-matrix least-squares refinement of $|F^2|$. An absorption correction was applied using the program XABS2.[17] Hydrogen atoms were included in calculated positions using a riding model with C−H distances of 0.96 Å and fixed isotropic thermal parameters of 0.08 Å^2. All non-hydrogen atoms were refined with anisotropic thermal parameters.

Results and Discussion

The synthesis of manganese corrolates can be achieved either *via* the base-induced oxidative cyclization of the linear tetrapyrrolic precursor 1,19-dideoxybiladiene-*a*,*c* in the presence of

(7) Goff, H. M. In *Iron Porphyrins*; Lever, A. B. P., Gray, H. B., Eds.; Adison-Wesley: London, 1983.
(8) Evans, D. F. *J. Chem. Soc.* **1959**, 2003.
(9) Sur, S. K. *J. Magn. Reson.* **1989**, *82*, 169.
(10) Ichimura, K.; Ichikawa, S.; Imamura, K. *Bull. Chem. Soc. Jpn.* **1976**, *49*, 1157.
(11) Johnson, A. W.; Kay, I. T. *J. Chem. Soc. C* **1965**, 1620.
(12) Grigg, R.; Johnson, A. W.; Shelton, G. *J. Chem. Soc. C* **1971**, 2287.
(13) Johnson, A. W.; Kay, I. T.; Markham, E.; Price, R.; Shaw, K. B. *J. Chem. Soc. C* **1959**, 3416.
(14) Fischer, H.; Orth, H. In *Die Chemie des Pyrrols*; Academische Verlag: Leipzig, Germany, 1934; Vol. I.
(15) Badger, G. M.; Harris, R. N. L.; Jones, R. A. *Aust. J. Chem.* **1964**, *17*, 1022.
(16) SHELXTL-Plus, Siemens Analytical Instruments, Madison, WI, 1994.
(17) Parkin, S. R.; Moezzi, B.; Hope, H. *J. Appl. Crystallogr.* **1995**, *28*, 53.

Table 1. Summary of Data Collection, Structure Solution, and Refinement Parameters for [(7,13-Me_2-HEC)Mn]

chem formula	$C_{33}H_{39}MnN_4$
mol wt	546.62
cryst description	red plate
cryst size, mm	0.6 × 0.3 × 0.3
a, Å	4.671(2)
b, Å	28.31(2)
c, Å	20.882(6)
β, deg	94.60(3)
V, Å^3	2753(2)
Z	4
space group	$P2_1/n$
d_{calc}, g/cm^3	1.319
linear abs/coeff, mm^{-1}	4.110
radiation	Cu Kα
T, K	293
θ range, deg	2.63−59.95
range of transm factors	0.08−0.29
no. of obs reflns	4088
no. of variables	344
*R*1,[a] w*R*2[b] [$I > 2\sigma(I)$]	0.0563, 0.1545
*R*1, w*R*2 (all data)	0.0816, 0.2029

[a] $R1 = \sum||F_o - F_c||/\sum|F_o|$. [b] $wR2 = [\sum[w(F_o^2 - F_c^2)^2]/\sum[w(F_o^2)^2]]^{1/2}$.

Table 2. Atomic Coordinates (×10^4) and Isotropic Thermal Parameters (Å^2 × 10^3) for [(7,13-Me_2-HEC)Mn]

	x	*y*	*z*	U(eq)[a] Å^2
Mn	5273(2)	1365(1)	7760(1)	48(1)
N(21)	4115(9)	728(1)	7740(2)	48(1)
N(22)	8195(8)	1248(1)	8430(2)	44(1)
N(23)	6050(8)	2020(1)	7685(2)	45(1)
N(24)	2306(8)	1390(1)	7089(2)	48(1)
C(1)	1963(11)	586(2)	7282(2)	50(1)
C(2)	1680(11)	89(2)	7331(2)	54(1)
C(2A)	−209(13)	−233(2)	6917(3)	70(2)
C(2B)	1175(18)	−412(3)	6337(3)	101(3)
C(3)	3653(12)	−61(2)	7824(3)	55(1)
C(3A)	4189(14)	−556(2)	8052(3)	68(2)
C(3B)	2985(16)	−684(2)	8678(3)	81(2)
C(4)	5182(11)	344(2)	8079(2)	49(1)
C(5)	7391(11)	396(2)	8564(2)	50(1)
C(6)	8768(10)	819(2)	8735(2)	43(1)
C(7)	11042(10)	896(2)	9233(2)	47(1)
C(7A)	12240(13)	531(2)	9688(3)	62(1)
C(8)	11790(10)	1361(2)	9218(2)	46(1)
C(8A)	13974(11)	1607(2)	9662(2)	56(1)
C(8B)	12768(16)	1759(2)	10280(3)	81(2)
C(9)	9998(10)	1585(2)	8716(2)	42(1)
C(10)	9941(10)	2059(2)	8537(2)	46(1)
C(11)	8090(10)	2268(2)	8064(2)	44(1)
C(12)	7978(11)	2754(2)	7866(2)	49(1)
C(12A)	9754(13)	3143(2)	8184(3)	61(1)
C(12B)	8458(16)	3346(3)	8759(3)	87(2)
C(13)	5926(11)	2792(2)	7365(2)	52(1)
C(13A)	5075(14)	3228(2)	6992(3)	70(2)
C(14)	4680(10)	2335(2)	7249(2)	47(1)
C(15)	2462(11)	2214(2)	6794(2)	53(1)
C(16)	1329(11)	1756(2)	6709(2)	50(1)
C(17)	−874(10)	1577(2)	6260(2)	55(1)
C(17A)	−2465(12)	1860(2)	5744(3)	70(2)
C(17B)	−750(15)	1947(3)	5169(3)	85(2)
C(18)	−1186(11)	1099(2)	6388(2)	58(1)
C(18A)	−3272(13)	777(3)	6030(3)	72(2)
C(18B)	−2403(18)	609(3)	5387(3)	104(3)
C(19)	883(11)	980(2)	6913(2)	50(1)

[a] *U*(eq) is defined as one-third of the trace of the orthogonalized $\mathbf{U}_{ij}$ tensor.

metal salts or by reaction of the preformed macrocyclic ring with a proper metal carrier such as manganese acetate in DMF or $Mn_2(CO)_{10}$ in toluene. Best yields have been obtained with the first synthetic procedure.

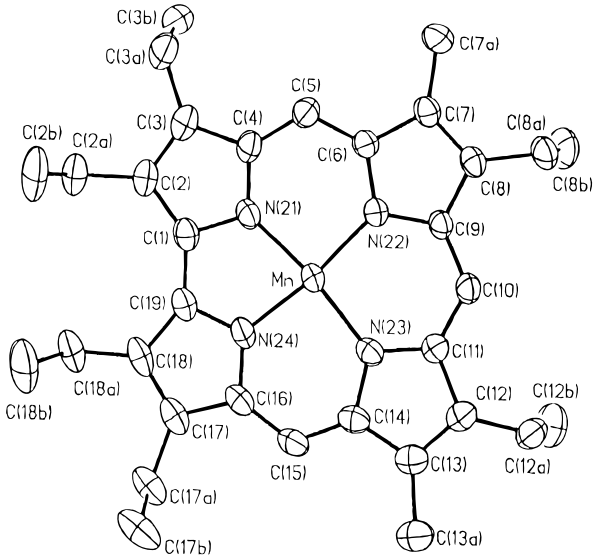

Figure 2. Computer-generated plot of [Mn(7,13-Me_2-HEC)] with the labeling scheme used. Ellipsoids are drawn for 50% occupancy. Hydrogen atoms have been omitted for clarity.

The XPS spectrum of the free ligand (H_3OMC) shows two N 1s peaks at BE 397.6 and 399.9 eV in a 1:3 ratio. The two signals can be assigned on the basis of their relative intensity and of literature data to pyrrole and aza type nitrogens, respectively.[1,18,19] The difference in BE is very close to that previously observed for porphyrins and phthalocyanines.[20] A single peak is observed in the spectrum of the complex [Mn(OMC)] at BE 398.7 eV: Such value has been previously interpreted as indication of a coordinative mode of all nitrogen atoms involving sp^2 N donors.[1,21] Both components ($^3/_2$, BE = 642.0 eV; $^1/_2$, BE = 652.6 eV) of the Mn 2p are in agreement with the +3 oxidation state of the metal ion, consistent with the trianionic nature of the ligand.[22]

The FAB mass spectra of all complexes (**1**−**7**) show the presence of the molecular peaks. The M/2e peaks are also present.

In the solid state [Mn(OMC)] has a magnetic moment, corrected for the diamagnetic ligand contribution, which value, $\mu = 4.76\ \mu_B$, is consistent with a high-spin state for the Mn(III) d^4 ion.

The synthesis of complex **6**, (7,13-dimethyl-2,3,8,12,17,18-hexaethylcorrolato)manganese(III), where the presence of six peripheral ethyl substituents dramatically improves the solubility, allowed us to grow crystals suitable for X-ray analysis. Figure 2 illustrates the geometry and the numbering scheme for the complex. Selected bond lengths and angles are reported in Table 3.

The tetraazamacrocyclic corrole moiety acts as a trianionic ligand for the Mn(III) atom which resides in an approximately square planar coordination environment. This is a very interesting feature of the structure: Such coordination behavior is highly unusual for Mn(III) derivatives[23] so that [Mn(7,13-Me_2-HEC)] represents, to the best of our knowledge, the first example of a "bare" Mn(III) tetrapyrrolic macrocycle complex. Manganese

(18) Zeller, M. V.; Hayes, R. G. *J. Am. Chem. Soc.* **1973**, *95*, 3855.
(19) Karveik, D.; Winograd, N.; Davis, D. G.; Kadish, K. M. *J. Am. Chem. Soc.* **1974**, *96*, 591.
(20) Niwa, Y.; Kobayashi, H.; Tsuchiya, T. *Inorg. Chem.* **1974**, *13*, 2891.
(21) Zanoni, R.; Boschi, T.; Licoccia, S.; Paolesse, R.; Tagliatesta, P. *Inorg. Chim. Acta* **1988**, *145*, 175.
(22) Uchida, K.; Soma, M.; Onishi, T.; Tamaru, T. *Inorg. Chim. Acta* **1978**, *26*, L3.
(23) Kemmit, R. D. W. In *Comprehensive Inorganic Chemistry*; Trotman-Dickenson, A. F., Ed.; Pergamon Press: Oxford, U.K., 1973.

Table 3. Important Bond Lengths (Å) and Angles (deg) in [(7,13-Me_2-HEC)Mn]

Mn−N(21)	1.882(4)	C(4)−C(5)	1.394(7)
Mn−N(23)	1.899(4)	C(5)−C(6)	1.395(7)
Mn−N(24)	1.891(4)	C(6)−C(7)	1.442(6)
Mn−N(22)	1.905(4)	C(7)−C(8)	1.365(7)
N(21)−C(4)	1.370(6)	C(8)−C(9)	1.435(7)
N(21)−C(1)	1.390(6)	C(9)−C(10)	1.392(7)
N(22)−C(9)	1.378(6)	C(10)−C(11)	1.392(7)
N(22)−C(6)	1.386(6)	C(11)−C(12)	1.437(7)
N(23)−C(11)	1.382(6)	C(12)−C(13)	1.364(7)
N(23)−C(14)	1.394(6)	C(13)−C(14)	1.431(7)
N(24)−C(16)	1.360(6)	C(14)−C(15)	1.392(7)
N(24)−C(19)	1.373(6)	C(15)−C(16)	1.407(7)
C(1)−C(2)	1.419(7)	C(16)−C(17)	1.427(7)
C(1)−C(19)	1.426(7)	C(17)−C(18)	1.389(8)
C(2)−C(3)	1.392(7)	C(18)−C(19)	1.441(7)
C(3)−C(4)	1.429(7)		
N(21)−Mn−N(23)	172.2(2)	C(14)−N(23)−Mn	126.8(3)
N(21)−Mn−N(24)	80.1(2)	C(16)−N(24)−C(19)	110.7(4)
N(23)−Mn−N(24)	92.1(2)	C(16)−N(24)−Mn	130.7(3)
N(21)−Mn−N(22)	92.1(2)	C(19)−N(24)−Mn	118.5(3)
N(23)−Mn−N(22)	95.7(2)	N(21)−C(1)−C(2)	107.7(4)
N(24)−Mn−N(22)	172.1(2)	N(21)−C(1)−C(19)	110.6(4)
C(4)−N(21)−C(1)	109.8(4)	C(2)−C(1)−C(19)	141.6(5)
C(4)−N(21)−Mn	131.2(3)	C(3)−C(2)−C(1)	107.1(4)
C(1)−N(21)−Mn	118.8(3)	C(2)−C(3)−C(4)	108.3(5)
C(9)−N(22)−C(6)	108.6(4)	N(21)−C(4)−C(5)	120.6(4)
C(9)−N(22)−Mn	125.1(3)	N(21)−C(4)−C(3)	107.1(4)
C(6)−N(22)−Mn	126.2(3)	C(5)−C(4)−C(3)	132.3(5)
C(11)−N(23)−C(14)	108.0(4)	C(6)−C(5)−C(4)	125.2(5)
C(11)−N(23)−Mn	125.3(3)	N(22)−C(6)−C(5)	124.5(4)
N(22)−C(6)−C(7)	107.7(4)	C(15)−C(14)−N(23)	124.4(5)
C(5)−C(6)−C(7)	127.8(4)	C(15)−C(14)−C(13)	127.6(4)
C(8)−C(7)−C(6)	107.7(4)	N(23)−C(14)−C(13)	108.0(4)
C(7)−C(8)−C(9)	108.0(4)	C(14)−C(15)−C(16)	124.5(5)
N(22)−C(9)−C(10)	123.6(4)	N(24)−C(16)−C(15)	121.5(4)
N(22)−C(9)−C(8)	108.1(4)	N(24)−C(16)−C(17)	107.7(5)
C(10)−C(9)−C(8)	128.3(4)	C(15)−C(16)−C(17)	130.8(5)
C(11)−C(10)−C(9)	126.7(4)	C(18)−C(17)−C(16)	107.4(5)
N(23)−C(11)−C(10)	123.4(4)	C(17)−C(18)−C(19)	107.4(4)
N(23)−C(11)−C(12)	108.3(4)	N(24)−C(19)−C(18)	106.7(5)
C(10)−C(11)−C(12)	128.2(4)	N(24)−C(19)−C(1)	111.9(4)
C(13)−C(12)−C(11)	107.7(4)	C(18)−C(19)−C(1)	141.3(5)

porphyrinates are in fact penta- or hexacoordinated: In the case of pentacoordinated derivatives, where the relatively short Mn−N bond distances (average 2.005 Å) have been related to the strong metal−porphyrin π interactions, the metal is displaced out of the macrocycle plane and a concomitant ruffling of the porphyrin core is observed. At variance with what observed in the case of different metal ions the addition of a sixth ligand to manganese porphyrinates does not always remove the displacement of the metal from the plane. The values of such displacements are as high as 0.12 Å for [Mn(TPP)Cl(Py)] and 0.086 Å for [Mn(TPP)N_3(CH_3OH)].[24]

In the structure of [Mn(7,13-Me_2-HEC)] the 23-atom core of the corrole ring has a planar conformation; the average deviation from their least-squares plane is 0.025 Å, with the largest deviation being 0.067 and 0.076 Å for C(2) and C(3), respectively. Such deviations are much smaller than those observed for other corrolates, *e.g.*, 0.1 Å in [Rh(OMC)$AsPh_3$], 0.22 Å in [Co(OMTPC)PPh_3], 0.164 Å in [(FeOEC)$_2$O], 0.193 Å in [Fe(OEC)Cl], 0.139 Å in [Fe(OEC)Ph], and 0.219 Å in [Fe(OEC)Py].[1]

Previous observations in the structures of penta- and hexacoordinated metallocorrolates showed that the metal atoms are diplaced 0.26−0.53 Å from the mean plane of the macrocycle while in the present structure the Mn atom is essentially in the plane, the maximum deviation observed being 0.031 Å. This behavior may be ascribed to the different coordination number of the metal atom; nonplanar conformations in fact result either from intramolecular repulsion of axial ligands with the atoms of the core or from packing in the crystal. In the present structure the presence of extended $\pi-\pi$ interactions (see below) also favors the planarity of the complex.

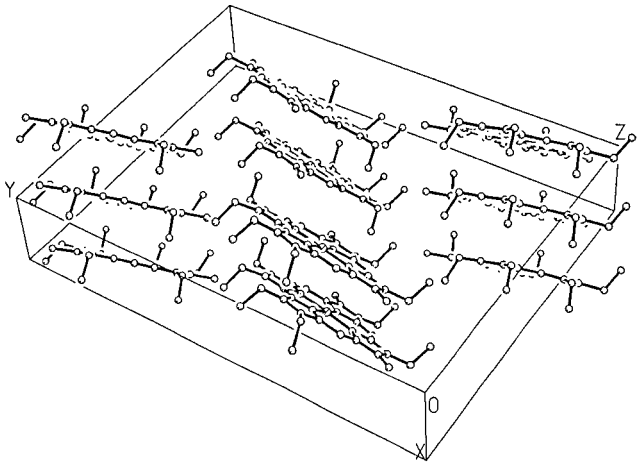

Figure 3. View of the molecular packing in the unit cell of [Mn(7,13-Me_2-HEC)].

The average Mn−N bond length is 1.894(4) Å. The presence of the direct link between the pyrroles A and D makes the four Mn−N bonds unequivalent, with the Mn−N(21) and Mn−N(24) bonds shorter than the corresponding Mn−N(22) and Mn−N(23); this feature has been previously reported in the literature for other metallocorrolates.[6,25]

The Mn−N bond distances, in addition, are significantly shorter than the corresponding ones in Mn(III) porphyrinates, where the average bond length is 2.0 Å. This shortening can be ascribed to the reduced hole size of the corrole ligand with respect to other macrocycles since a similar decrease of the metal−nitrogen bond lengths was observed for [Rh(OMC)$AsPh_3$], where the average Rh−N bond length is 1.945 Å vs 2.032 Å in [Rh(OEP)CH_3],[6] and [Co(OMTPC)PPh_3], where the average Co−N bond length is 1.888 Å vs 1.982 Å reported for Co(III) porphyrinates.[24,25]

This relatively short Mn−N bond distance reveals, however, that the strong metal−π system interaction present in Mn(III) porphyrinates is still present, if not even enhanced, in manganese corrolates.

The molecular packing of [Mn(7,13-Me_2-HEC)] is characterized by a strong overlap of the π-systems with the formation of infinite stacks of molecules (Figure 3).

Scheidt and Lee[26] have given a detailed analysis of the $\pi-\pi$ interactions for porphyrin systems, indicating the geometric parameters necessary for their characterization. These parameters are the mean plane separation (MPS), the center-to-center (Ct−Ct) distances, and the lateral shift (LS) between the macrocycles. According to these values, $\pi-\pi$ interactions can be grouped into three types as weak, intermediate, and strong.

The [Mn(7,13-Me_2-HEC)] aggregates show a value of 3.33 Å for the MPS with a Ct−Ct of 4.671 Å and a LS of 3.28 Å, with a consequent slip angle (the angle between the mean plane and the Ct−Ct axis) of 44.6°. Such structural characteristics

(24) Scheidt, W. R. In *The Porphyrins*; Dolphin, D. H., Ed.; Academic Press: New York, 1978.

(25) Paolesse, R.; Licoccia, S.; Bandoli, G.; Dolmella, A.; Boschi, T. *Inorg. Chem.* **1994**, *33*, 1171.

(26) Scheidt, W. R.; Lee, Y. J. In *Metal Complexes with Tetrapyrrole Ligands I*; Buchler, J. W., Ed.; Springer-Verlag: Berlin and Heidelberg, Germany, 1987.

Table 4. Optical Data for [Mn(OMC)]

solvent	λ_{max}, nm ($\epsilon \times 10^4$)		
chloroform	408 (3.15)	588 (0.76)	
benzene	404 (3.08)	590 (0.74)	
THF	386 (3.30)	479 (1.01)	585 (0.95)
pyridine	392 (3.15)	485 (1.09)	591 (0.97)

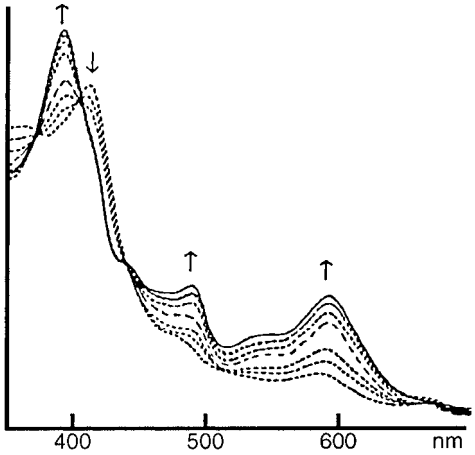

Figure 4. Changes in the electronic absorption spectra of [Mn(OMC)] in chloroform upon addition of pyridine. The bottom trace refers to the spectrum in chloroform, and the top trace, to that in neat pyridine.

define [Mn(7,13-Me_2-HEC)] existing as aggregates of intermediate strength.

It is relevant to note that the presence of the direct pyrrole−pyrrole link does not prevent the formation of extended $\pi-\pi$ interactions and that the aggregates are arranged in an ordered way, with the direct pyrrole−pyrrole link pointing to the same side of the columnar stacks.

This is the first example of extended stacked arrangements for a corrole complex: $\pi-\pi$ interactions have been reported in the solid state for iron corrolates, but the presence of axial ligands limited the interactions to the formation of dimers.[27]

The electronic absorption spectra of manganese alkylcorrolates are strongly solvent dependent. Table 4 reports as an example data relative to [Mn(OMC)]. In noncoordinating solvents the spectra are characterized by two main absorptions: a Soret-like band centered around 400 nm and a weaker band around 590 nm, both deriving from transitions within the π system of the macrocycle.[28]

In coordinating solvents, such as THF or pyridine, the Soret band is shifted to higher energies and an additional band at 480 nm is present. In order to clarify the nature of the spectral variations observed, the reactions of [Mn(OMC)] with various nitrogenous bases (pyridine, 4-methylpyridine, 4-vinylpyridine) have been studied spectrophotometrically. Spectral variations relative to the reaction with pyridine are shown in Figure 4. The presence of clear isosbestic points indicate the occurrence of a single ligand addition process.

Analysis of the data has been carried out using plots of log $\alpha/(1-\alpha)$ versus log [L], where [L] is the nitrogenous base concentration and α is the fraction of bound complex. In all cases only one molecule of base is axially ligated to manganese and the equilibrium constants for the formation of [Mn(OMC)L] complexes resulted to be $K = 14.8\ M^{-1}$, $K = 80.5\ M^{-1}$, and $K = 6.5\ M^{-1}$ for pyridine, 4-methylpyridine, and 4-vinylpiridine, respectively. No direct relationship with the axial ligand basicity has been observed. The low values of the equilibrium constants together with the observation that axial coordination occurs only for great ratios [Mn]:[L] indicate that the equilibria are shifted toward the unligated forms where the drive of manganese for pentacoordination is probably satisfied by the interactions between different macrocycles.

It has been suggested that the symmetrical d^5 electronic configuration favors the Mn(II) state and a [$Mn^{II}P^{\bullet+}$] formulation has been proposed for manganese coordinated to a porphyrin.[29] Also, in the case of Mn(II) porphyrinates oxidation of the ligand to a porphyrin cation radical resulted to be much easier than that of the metal ion. The first ring oxidation occurs in fact at much lower potential than that of the corresponding Zn(II) complex (+0.06 V for [Mn(TPP)] vs +0.99 V for [Zn(TPP)]) while the first metal-centered oxidation for [Mn(TPP)] occurs at +1.75 V.[29]

More recently[30] detailed analysis of the optical and NMR spectra of several manganese porphyrinates lead to the conclusion that an axial ligand dependent valence state isomerization occurs for such complexes and that their electronic ground state can be described as a mixture of [$Mn^{II}P^{\bullet+}$] and [$Mn^{III}P$] as a function of the axial ligand. The optical spectrum of [Mn(TPP)-ClO_4], for which the [$Mn^{II}P^{\bullet+}$] formulation is considered to be dominant, is almost identical to that of the cation radical generated by electrochemical oxidation of manganese porphyrinates.[31] A general feature of these spectra is the increase in intensity in the long wavelength spectral region, the same feature observed for manganese corrolates in pyridine.

Electronic rearrangements of metal complexes of tetrapyrrolic macrocycles induced by axial ligation have been reported to occur by several investigators. Beside the manganese porphyrins quoted (see above) reduction of ferric porphyrins in solution has been observed in the presence of several ligands such as cyanide, piperidine, phosphines, *etc*.[32] The mechanism of such reactions is believed to be the same for a variety of axial ligands and involves intramolecular electron transfer to give Fe(II) species and ligand radicals. The rates of the reactions are strongly dependent on the substituent pattern on the macroring.[33] Furthermore, coordination of *t*-buNC to Fe(III) isobacteriochlorin has been reported to induce a reversible electron rearrangement resulting in the reduction of Fe(III) to Fe(II) and the simultaneous oxidation of the macrocycle to a π-cation radical.[34] Finally, electronic rearrangements caused by axial ligation of pyridine have been reported to occur also in the case of manganese complexes of phthalocyanines.[35] The optical spectra of these complexes show additional bands, and this feature has been attributed to the formation of two electronic isomers of [Mn(Pc)], [$Mn^{I}(PC^{\bullet+})Py$] and [$Mn^{III}(Pc^{\bullet-})Py_2$], generated by intramolecular charge transfer induced by mono and bis coordination of pyridine.

The ligands can strongly influence the redox properties of the metal ion: the metal interacts with its environment

(27) Vogel, E.; Will, S.; Schulze Tilling, A.; Neumann, L.; Lex, J.; Bill, E.; Trautwein, A. X.; Wieghardt, K. *Angew. Chem., Int. Ed. Engl.* **1994**, *33*, 731.
(28) Hush, N. S.; Dyke, J. M.; Williams, M. L.; Woolsey, I. S. *J. Chem. Soc., Dalton Trans.* **1974**, 395.
(29) Richert, S. A.; Tsang, P. K. S.; Sawyer, D. T. *Inorg. Chem.* **1988**, *27*, 1814.
(30) Turner, P.; Gunter, M. J. *Inorg. Chem.* **1994**, *33*, 1406.
(31) Goff, H. M.; Phillippi, M. A.; Boersma, A. D.; Hansen, A. P. *Adv. Chem. Ser.* **1982**, *No. 201*, 357.
(32) Walker, F. A.; Simonis, U. In *NMR of Paramagnetic Molecules*; Berliner, L. J., Reuben, J., Eds.; Plenum Press: New York, 1993; and references therein.
(33) White-Dixon, D.; Barbush, M.; Shirazi, A. *Inorg. Chem.* **1985**, *24*, 1081.
(34) Walker, F. A.; Simonis, U. In *Encyclopedia of Inorganic Chemistry (Iron Porphyrin Chemistry)*; Bruce King, R., Ed.; John Wiley & Sons: New York, 1994.
(35) Dolotova, O. V.; Bundina, N. I.; Derkacheva, V. M.; Negrimovskii, V. M.; Minin, V. V.; Larin, G. M.; Kaliya, O. L.; Luk'yanets, E. A. *Zh. Obshch. Khim.* **1992**, *62*, 2064.

modifying its inherent redox tendencies. Corrole has a stronger equatorial ligand field with respect to other macrocycles which contributes to increased electron density at the metal. It is a stronger base and it is easier to oxidize than other tetrapyrroles. In the case of Co(III) and Rh(III) derivatives the first ring-centered oxidation occurs at a potential which is ca. 800 mV more negative with respect to analogous porphyrin complexes in agreement with the trianionic nature of the corrole ligand and the high electron density at the metal center.[1] Also, in the case of [Fe(OEC)NO] the first oxidation occurs at the macrocycle generating an iron(II) nitrosyl corrole π-cation radical, while in the case of iron nitrosyl porphyrinates the same oxidation occurs at the metal center.[36]

The possibility that the pyridine adducts of manganese corrolates could be formulated as [Mn^{II}corrole$^{\bullet+}$)Py] derived from intramolecular ligand to metal electron transfer is supported by the presence of the additional band at 480 nm in their electronic spectra that can be attributed to a metal to ligand charge transfer transition. The relative intensity of this band is in fact related to the electron withdrawing−donating ability of the peripheral substituents on the macrocycle; thus, the intensity decreases going from [Mn(7,8,12,13-TMC)Py] ($\epsilon = 1.40 \times 10^4$) to [Mn(OMC)Py] ($\epsilon = 1.09 \times 10^4$) to [Mn(7,13-$Me_2$-HEC)Py] ($\epsilon = 1.02 \times 10^4$). When an electron-withdrawing substituent such a formyl group is present at the 10-position, the intensity of the band is further enhanced [$\epsilon = 1.72 \times 10^4$ for (10-formyl-2,3,17,18-tetraethyl-7,8,12,13-tetramethylcorrolato)manganese-(II)] in agreement with a lower electron density at the macrocycle.[37]

In order to verify the formulation of the pyridine adducts of manganese corrolates as [Mn^{II}corrole$^{\bullet+}$) EPR and ^{1}H NMR spectra of the complexes have been examined.

The EPR spectrum of [Mn(7,13-Me_2-HEC)Py] at $T = 100$ K is shown in Figure 5b ($c = 5 \times 10^{-3}$ M) while Figure 5d shows an enlargement of the region around $g = 2$. The spectrum shows an intense resonance, centered at $g = 2$, displaying the six-line hyperfine splitting (average spacing 87 G) typical of monomeric Mn(II) complexes.[38,39] A very weak signal is also present in the low-field region of the spectrum. Similar broad resonances have been reported for dimeric Mn-(II) species or for distorted monomeric complexes.[39−42] Since the intensity of the resonance varies as a function of the sample concentration (relative intensity of the resonance with respect to the main signal at $g = 2$ varies from 1:10 to 1:25 to 1:100 going from 5×10^{-2} M to 5×10^{-3} M to 5×10^{-4} M as shown in traces a−c in Figure 5), it can be attributed to the persistence of $\pi-\pi$ interactions in solution with the formation of dimeric aggregates.

Such observations demonstrate that the metal ion is in the +2 oxidation state and strongly support the formulation of the complex as the valence tautomer [Mn^{II}(7,13-Me_2-HEC$^{\bullet+}$)Py].

EPR was silent at room temperature. This is not an unusual feature for tetrapyrrolic macrocycles π cation radicals[30,31] and can be attributed to enhanced electron spin relaxation rate caused by spin−spin magnetic interaction between the ligand radical and the metal ion. This is in agreement with a radical generated through electron transfer to the coordinated manganese ion. In the case of the valence isomers generated by reaction of pyridine with [Mn(Pc)] no spectrum was observed at room temperature and no signals of the Pc radicals have been observed at −196 °C. The absence of these signals has been attributed to the fact that radicals trapped in glasses at low temperature show weak broadened signals undetectable against the background of the intense spectrum due to Mn(II).[35]

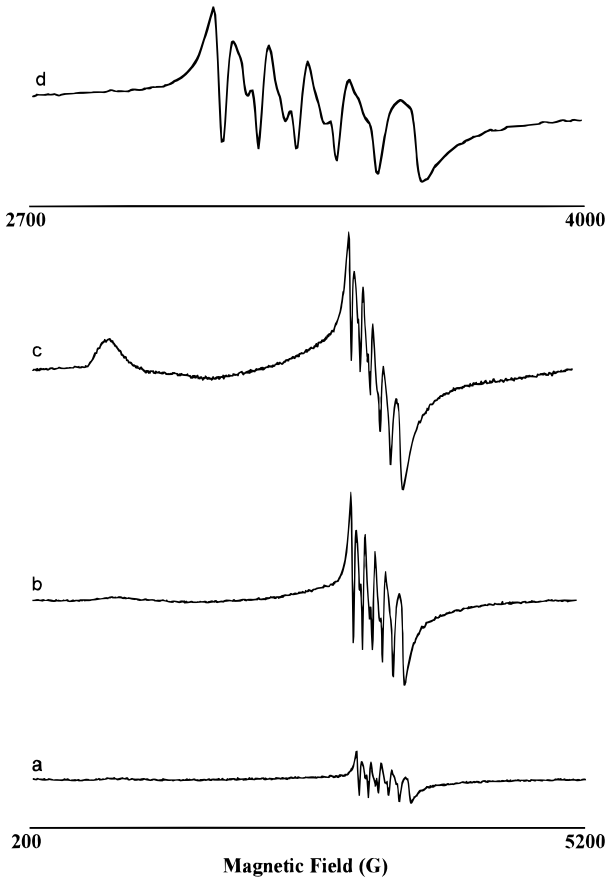

Figure 5. EPR spectra of [Mn(7,13-Me_2-HEC)] in pyridine: (a) 5×10^{-4} M; (b) 5×10^{-3} M; (c) 5×10^{-2} M; (d) expansion of the region around $g = 2$ in spectrum *b*.

The ^{1}H NMR spectrum of [Mn(OMC)Py] is shown in Figure 6a and reveals four isotropically shifted resonances of equal intensity (labeled A−D) that are clearly due to the methyl peripheral substituents. Systematic substitution of two symmetrical methyl groups with ethyls lead to the assignments reported in Table 5. The weaker peaks labeled X and Y have been attributed to the 5,15-H and 10-H, respectively, on the basis of their intensity and by comparison with the spectrum of the 5,15-deuteriated derivative [Mn(5,15-^{2}H-Et_2-HMC)] (insert in Figure 6). No peaks upfield of TMS have been observed.

The large isotropic shift of all the resonances is indicative of electronic delocalization on the macrocycle π system and suggests a dominant contact contribution to the shifts. This indication is confirmed by the large upfield shift observed for the resonances of the β-pyrrole hydrogens in the spectrum of [(Mn(TMC)Py] (Table 5). The temperature dependence of the isotropic shifts for [Mn(OMC)Py] has also been examined and gives rise to linear Curie plots indicating the absence of sizable dipolar contribution and of spin and/or chemical equilibria.[2,43]

It is well-known that the isotropic shifts observed for manganese porphyrinates are relatively small and dominated

(36) Autret, M.; Will, S.; Van Caemelbecke, E.; Lex, J.; Gisselbrecht, J. P.; Gross, M.; Vogel, E.; Kadish, K. M. *J. Am. Chem. Soc.* **1994**, *116*, 9141.
(37) Paolesse, R. Manuscript in preparation.
(38) Brudvig, G. W. In *Advanced EPR. Applications in Biology and Biochemistry*; Hoff, A. J., Ed.; Elsevier: Amsterdam, 1989.
(39) Policar, C.; Artaud, I.; Mansuy, D. *Inorg. Chem.* **1996**, *35*, 210.
(40) Mabad, B.; Cassoux, P.; Tuchagues, J. P.; Hendrickson, D. N. *Inorg. Chem.* **1986**, *25*, 1420.
(41) Mathur, P.; Crowder, M.; Dismukes, G. C. *J. Am. Chem. Soc.* **1987**, *109*, 5227.
(42) Pessiki, P. J.; Khangulov, S. V.; Ho, D. M., Dismukes, G. C. *J. Am. Chem. Soc.* **1994**, *116*, 891.

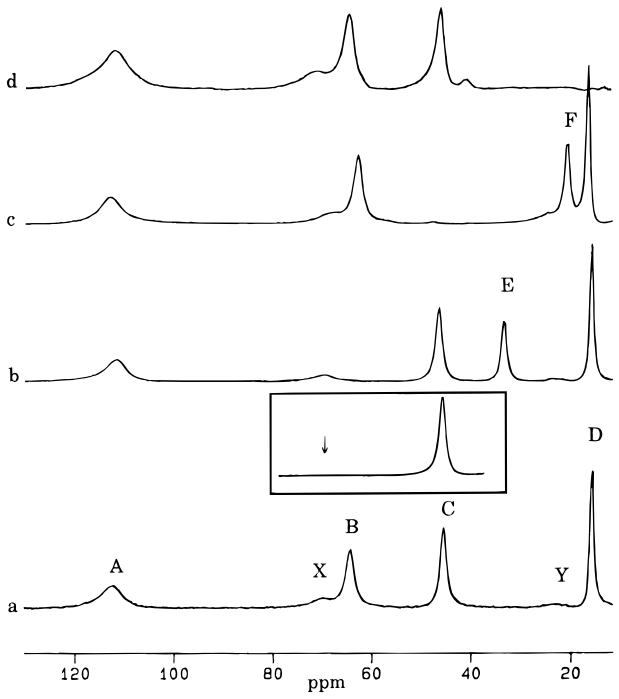

Figure 6. 400 MHz ^{1}H NMR spectra of manganese corrolates in pyridine-d_5: (a) [Mn(OMC)]; (b) [Mn(8,12-Et$_2$-NMC)]; (c) [Mn(3,17-Et$_2$-HMC)]; (d) [Mn(7,13-Et$_2$-HMC)]. Insert shows the effect of deuteration in positions 5 and 15.

by contact interaction reflecting extensive porphyrin to metal π-bonding.[43,44] The large spread of shifts observed for all the resonances in the spectra of manganese corrolates together with the high relaxation rates determined suggests the formation of a corrole cation-radical *via* ligand-to-metal charge transfer.[45] Similar downfield shifts for β-methyls and *meso*-hydrogens have been previously observed in the case of iron complexes of porphyrin, chlorin, and isobacteriochlorin π-cation radicals.[46−48] Solution magnetic susceptibility measurements have been performed at 293 K ($\mu = 3.60\ \mu_B$) and 235 K ($\mu = 3.02\ \mu_B$), near the solution freezing point. The results are indicative of antiferromagnetic coupling between an intermediate spin Mn(II) ($S = {}^3/_2$) ion and the corrole radical ($S = {}^1/_2$). It is noteworthy that the intermediate ($S = {}^3/_2$) spin state was that determined for the valence isomers of manganese porphyrinates

(43) (a) La Mar, G. N.; Walker, F. A. *J. Am. Chem. Soc.* **1975**, *97*, 5103. (b) La Mar, G. N.; Walker, F. A. In *The Porphyrins*; Dolphin, D. H., Ed.; Academic Press: New York, 1978.
(44) Hill, C. L.; Williamson, M. L. *Inorg. Chem.* **1985**, *24*, 2836.
(45) La Mar, G. N.; Walker, F. A. *J. Am. Chem. Soc.* **1973**, *95*, 6950.
(46) Fujii, H.; Ichikawa, K. *Inorg. Chem.* **1992**, *31*, 1110.
(47) Goff, H. M.; Phillippi, M. A. *J. Am. Chem. Soc.* **1983**, *105*, 7567.
(48) Ozawa, S.; Fujii, H.; Morishima, I. *J. Am. Chem. Soc.* **1992**, *114*, 1548.

Table 5. ^{1}H NMR Data for Manganese Corrolates in Pyridine, Where Labels Refer to Figure 6

label	δ, ppm	assgmt	$T_1 \pm 10\%$, ms	$T_2 \pm 10\%$, ms
A	112.4 (6 H)	2,18-CH_3	0.98	0.13
B	64.3 (6 H)	8,12-CH_3	1.23	0.30
C	45.5 (6 H)	3,17-CH_3	2.92	0.59
D	15.8 (6 H)	7,13-CH_3	3.76	1.00
X	70.5 (2H)	5,15-H	*a*	*a*
Y	25.0 (1 H)	10-H	*a*	*a*
E	35.6 (4 H)	8,12-$CH_2$$CH_3$	*a*	0.60
F	21.5 (4 H)	3,17-$CH_2$$CH_3$	*a*	0.53
	55.0 (4H)	2,18-$CH_2$$CH_3$	*a*	0.31
	ca. 8[b]	7,13-$CH_2$$CH_3$	*a*	*a*
	3.3 (6 H)	2,18-CH_2CH_3	*a*	*a*
	3.0 (6 H)	3,17-CH_2CH_3	*a*	*a*
	2.9 (6 H)	7,13-CH_2CH_3	*a*	*a*
	2.9 (6H)	8,12-CH_2CH_3	*a*	*a*
	−40.0 (2 H)	3,17-H	*a*	0.23
	−123.0 (2 H)	2,18-H	*a*	0.09

[a] Not determined. [b] Obscured by solvent residual signals.

[$Mn^{II}P^{\bullet+}$].[30] The pattern observed in the EPR spectrum of [Mn(OMC)Py] can be attributed to Mn(II) with zero-field splitting due to the reduced symmetry of the metal ion binding site. The X-ray crystal structure reported for a similar complex, [Fe(OEC)Py],[1] shows that the coordinative environment of the metal atom is that of an approximately square pyramidal geometry with the macrocycle exhibiting large deviation from planarity (maximum distance of C and N atoms from the mean plane of the ring being 0.219 Å *vs* 0.077 Å for [Fe(OEC)Ph]). In this case ($D \ll h\nu$) the only transition observable is the m_s $+{}^1/_2 \rightarrow m_s$ $-{}^1/_2$ that remains fairly sharp while the m_s $+{}^5/_2 \leftrightarrow$ m_s $\pm{}^3/_2$ and m_s $\pm{}^3/_2 \leftrightarrow m_s$ $\pm{}^1/_2$ transitions are expected to be very broad.[38]

Finally, theoretical calculations will be needed to give more rigorous support to the conclusions derived from the experimental chemistry of metal corrolates.

Acknowledgment. Thanks are due to Professor M. Paci (University of Rome Tor Vergata) and to Dr. Manlio Occhiuzzi (University of Rome La Sapienza) for helpful discussions. The valuable technical assistance of Ms. C. D'Ottavi, Ms. S. Mini, and Mr. F. Bertocchi is gratefully acknowledged. This work has been supported by MURST and the CNR (Italy) and by the Deutsche Forschungsgemeinschaft (Se543/2-1) and the Fonds der Chemischen Industrie.

Supporting Information Available: Listings of data collection parameters and complete bond lengths, bond angles, anisotropic thermal parameters, and hydrogen coordinates and *U* values (Tables SI−SV) and Figures A and B, showing a side view of the molecule illustrating its planarity and a side view of [Mn(7,13-Me$_2$-HEC)] stacks (6 pages). Ordering information is given on any current masthead page.

IC960334I